

# SPAN-RATIO ANALYSIS USED TO ESTIMATE EFFECTIVE LIFT:DRAG RATIO IN THE DOUBLE-CRESTED CORMORANT *PHALACROCORAX AURITUS* FROM FIELD OBSERVATIONS

By C. J. PENNYCUICK

*Department of Biology, University of Miami, PO Box 249118, Coral Gables, FL 33124, USA*

*Accepted 15 September 1988*

## Summary

A method is described for measuring the effective lift:drag ratio of a bird in flapping flight from the bird's span ratio; that is, the ratio of the wing span in the upstroke to that in the downstroke. The method depends on the assumptions that the circulation on the wing is constant, and that the lift varies in proportion to the span. With some simplifications, it can be applied in the field to birds that cruise in steady, continuous flapping flight. Double-crested cormorants, observed on foraging flights, flew at a mean airspeed of  $14.7 \text{ m s}^{-1}$ , with a span ratio of 0.70. The effective lift:drag ratio, taking account of mechanical components of power only, was estimated to be 14.8. A much lower estimate (8.96) was obtained from a power curve program (Pennycuick, 1989). The discrepancy could be due (at least partly) to bias in the observations, but it is also suggested that one or more of the default values, used in the program for calculating induced, profile and parasite power, may be in need of downward revision.

## Introduction

A method for calculating the power required by a flying bird, as a function of its forward speed was published by Pennycuick (1975), but it is difficult to check the accuracy of the predictions. Traditionally, such comparisons have relied on physiological methods, involving the measurement of respiratory activity, or the consumption of food. Such an approach has the disadvantage that it measures the consumption of total fuel energy, whereas mechanical calculations estimate the mechanical power output required from the flight muscles. There are uncertainties in the conversion of fuel energy into mechanical work and, besides, it is difficult to separate energy consumption due to various components of mechanical effort from the animal's total power consumption.

Mechanical observations permit a more direct comparison of observed and estimated power. For example, the energy of vortex rings generated by slow-flying pigeons has been used to calculate induced power (Spedding, 1981; Spedding *et al.*

Key words: bird, flight, vortex, wake.

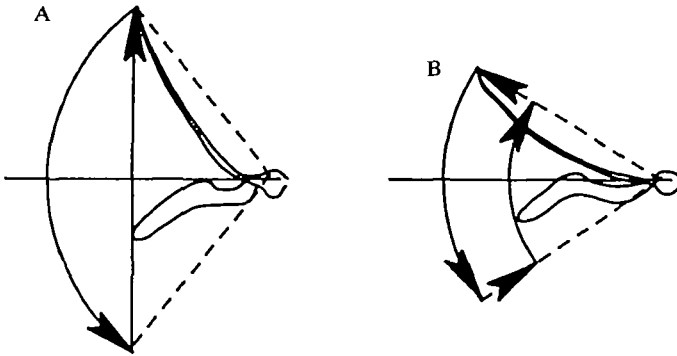


Fig. 1. (A) Motion assumed in Rayner's (1986) theory of the constant-circulation wake – wing span constant during downstroke, varying during upstroke. (B) Present theory – wing span constant during upstroke.

1984). Methods of this type are technically demanding, and capable of producing only limited amounts of data, on species that can be tested under laboratory conditions. However, observations made using similar methods, of the vortex wake of a kestrel (Spedding, 1981, 1987), have opened the possibility of making quantitative measurements in the field on a wider range of species. The vortex wake of the kestrel, flying level at cruising speed, was found to consist of a pair of continuous, undulating wing tip vortices, whose circulation was the same on the upstroke as on the downstroke. However, the vortices were further apart on the downstroke than on the upstroke, because the bird extended its wings fully on the downstroke, but shortened them by flexing the elbow and wrist joints on the upstroke. The basic principle of propulsion with such a 'concertina wake' has been explained with a qualitative discussion of the reasons why cruising flight is likely to be more economical with this type of wing action, than if the wing length is kept the same on both the upstroke and the downstroke (PennyCUICK, 1988). Although it does not appear practical to observe the actual values of lift and thrust in the field, the principle of the constant-circulation wake opens the possibility that the *ratio* of lift to thrust might be measurable in terms of the amount of shortening of the wing observed during the upstroke. This lift:thrust ratio is predicted by the existing methods of performance estimation (noted above), and is closely related to the amount of energy consumed in flying unit distance and, hence, to the energetic cost of migratory and foraging flights. A method of measuring it in the field would be of great interest.

#### *Rayner's analysis*

Expressions for the lift and thrust developed by a wing developing a constant-circulation wake have been given in a more quantitative analysis of different wake types (Rayner, 1986). To do so, Rayner simplified the motion in the manner indicated in Fig. 1A. The flapping motion is assumed to be sinusoidal in time, and symmetrical in amplitude, with equal angular deflections of the wing above and

below the horizontal plane. The wing is assumed to be fully stretched out during the downstroke, so that the wing tip describes an arc as shown. On the upstroke, the wing tip is assumed to follow a vertical straight line, achieved by shortening the wing progressively until it reaches the horizontal position, and then lengthening it until full stretch is achieved at the fully up position. This theoretical motion bears a general resemblance to the actual motion seen in slowed-down films of flying birds, although it is difficult to judge how closely the various assumptions correspond to reality in any particular bird. The ratio of lift to thrust can be estimated by dividing Rayner's (1986) equation 6 (for lift) by his equation 7 (for thrust). The resulting expression unfortunately contains a variable  $\gamma_1$ , which represents the spanwise distribution of lift along the wing. From Rayner's assumptions it follows that this variable occurs in the expression for the thrust, but not in that for the lift, so it cannot be eliminated by dividing one by the other. The shape of the lift distribution, which determines the value of  $\gamma_1$ , can only be conjectured. Rayner does not supply any values corresponding to lift distributions that might be considered probable.

#### *Span-ratio method*

The difficulty can be avoided by abandoning Rayner's starting assumptions, and substituting a motion like that shown in Fig. 1B. First, the assumption of sinusoidal motion is not good for low-speed flight (Pennycuick & Lock, 1976) and is not known to be any better for cruising flight. It is just as plausible to assume that the wing accelerates quickly, then maintains a steady angular velocity throughout most of the downstroke. Then, at the bottom of the downstroke, it reverses quickly and shortens, as in Fig. 1B, maintaining the reduced wing length until the top of the upstroke, when the wing lengthens once again to its full extent. This motion would not be easy to distinguish visually from that proposed by Rayner, and is equally reconcilable with such limited empirical information as exists. The difference is that the wing span is constant throughout the upstroke, instead of varying continuously as in Rayner's scenario. This assumption permits the ratio of lift to thrust to be related to the *span ratio*, that is the ratio of the wing span during the upstroke to that during the downstroke. The form of the spanwise lift distribution is not required, although it is assumed (as also in Rayner's version) that the shape of the spanwise lift distribution is the same on the upstroke as on the downstroke.

#### *The ratio of lift to thrust*

The basic mechanics of level flight with the 'concertina' type of wing action have been explained by Pennycuick (1988, 1989). If the circulation of the wingtip vortices remains constant throughout the cycle, as observed for the kestrel (Spedding, 1987), and if the spanwise lift distribution is the same on the upstroke as on the downstroke, then the lift developed by the wing is proportional to its span. The lift force is not necessarily directed upwards, but is defined as the component of the total aerodynamic force that acts at right angles to the incident

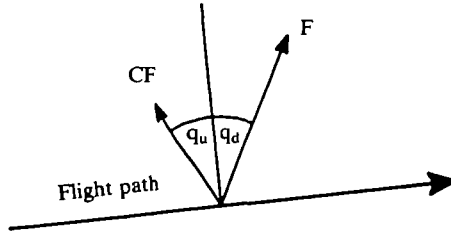


Fig. 2. Forces assumed in deriving equations 1 and 2.

air flow. During the downstroke the lift force is inclined forwards, whereas during the upstroke it is inclined backwards, and its magnitude is smaller. The weight is supported by the vertical component of the lift in both the upstroke and the downstroke, whereas the thrust results from the forward horizontal component in the downstroke being larger than the backward horizontal component in the upstroke.

Fig. 2 shows the forces assumed to be acting on a bird's wings during the upstroke and downstroke. The flapping cycle has been simplified to the extent that it is assumed to consist of two phases, the downstroke, lasting a time  $t_d$ , and the upstroke, lasting a time  $t_u$ . During each phase, it is assumed that a constant force is exerted, at a constant angle to the flight path. The flight path is not required to be horizontal, and could be inclined upwards or downwards. During the downstroke, a lift force ( $F$ ) is exerted, angled forwards, relative to the normal to the flight path, at an angle  $q_d$ . During the upstroke, a smaller force is exerted, angled backwards at an angle  $q_u$ . Under these assumptions, the magnitude of this force is  $CF$ , where  $C$  is the span ratio ( $C < 1$ ). The 'mean lift' ( $L$ ) is the force, averaged over a wingbeat cycle, exerted in a direction normal to the flight path (not necessarily vertically upwards) and the 'mean thrust' ( $T$ ) is the mean force exerted forwards along the flight path. From Fig. 2, we can write:

$$L = (t_d F \cos q_d + t_u CF \cos q_u) / (t_d + t_u), \quad (1)$$

$$T = (t_d F \sin q_d - t_u CF \sin q_u) / (t_d + t_u). \quad (2)$$

Two simplifying assumptions are now introduced. First, it is assumed that  $t_d = t_u$ . This might not be satisfactory for all birds, but for the study species, under the restricted conditions of steady cruising flight, the downstroke and upstroke did have approximately equal durations (see below). Second, it is assumed that  $q_d = q_u$ , and that both may be replaced by a single angle, the *lift angle* ( $q$ ). The justification for this is that the force depicted in Fig. 2 is the lift force on the wing, deriving from the circulation. The lift force is the component of the resultant aerodynamic force directed perpendicular to the relative airflow. Of course, the direction of the relative airflow varies with spanwise position along the wing, and the force shown in Fig. 2 is a vector average. If the durations of up- and downstrokes are equal, the lift can reasonably be assumed to be inclined backwards on the upstroke, by the same amount that it is inclined forwards on the

downstroke. These assumptions allow equations 1 and 2 to be simplified as follows:

$$L = [F(1 + C)\cos q]/2, \quad (3)$$

$$T = [F(1 - C)\sin q]/2. \quad (4)$$

Combining the two equations, we get:

$$L/T = [(1 + C)/(1 - C)]/\tan q. \quad (5)$$

If the flight path is horizontal, and the speed is constant, then the mean lift equals the bird's weight, and the mean thrust equals its drag. Under these conditions, the ratio estimated by equation 5 is the same as the 'effective lift: drag ratio' as defined by Pennycuick (1975), and here designated by  $N$ . It is defined as:

$$N = mgV/P, \quad (6)$$

where  $m$  is the body mass,  $g$  is the acceleration due to gravity, and  $P$  is the *mechanical* power output of the muscles required to maintain a steady airspeed  $V$ . In this context,  $P$  does not include metabolic components of power, as in the modified theory of Pennycuick (1975). To obtain an estimate of  $N$  (that is,  $L/T$ ) from equation 5, measurements are needed of just two variables, the span ratio ( $C$ ) and the lift angle ( $q$ ). These were obtained from video recordings and ornithodolite observations as follows.

## Materials and methods

### *Study species and site*

The double-crested cormorant *Phalacrocorax auritus* (Lesson) is a common, resident, breeding species around the coast of South Florida. Body measurements are given in Table 1. These cormorants typically roost communally, and make foraging flights up to a few kilometres between the roost and the feeding grounds. These flights are made in continuous flapping flight (not flap-gliding). Unlike plunge-diving species such as brown pelicans, double-crested cormorants do not usually cast about, searching for prey from the air, but proceed at a steady speed to an identifiable destination. The study site was at Sandy Key, which is located about 11 km south of East Cape Sable (the southwestern extremity of the Florida mainland), just within the southwestern boundary of the Everglades National Park. This small mangrove island is a nesting site for cormorants and other water birds, and is also used year-round as a roost. At certain times of day and states of the tide, a continuous stream of birds may be seen coming in or departing, to or from the feeding grounds. The writer's 6.7 m Helsen sailing boat was used for access to Sandy Key, and also as an observation platform.

### *Airspeed measurements*

For airspeed observations, the boat, which had a retractable swing-keel, was stranded at low tide on a conveniently situated sandbank between the north end of

Table 1. *Observed and calculated values*

Body measurements	
Mass (m)	1.41 kg
Wing span (b)	1.16 m
From field data	
Mean airspeed (V)	14.7 m s <sup>-1</sup>
Wingbeat frequency (f)	4.79 Hz
Span ratio (C)	0.70
Flapping wavelength ( $\lambda$ )	3.07 m
Up-angle	33.2°
Down-angle	28.0°
Vertical excursion of wing tip (h)	0.59 m
Lift angle upper limit (q)	21.0°
Effective lift: drag ratio (N)	14.8
From power curve calculation	
Minimum power speed (V <sub>mp</sub> )	11.4 m s <sup>-1</sup>
Maximum range speed (V <sub>mr</sub> )	18.5 m s <sup>-1</sup>
Effective lift: drag ratio (N)	8.96

The power curve calculation is based on suggested default values from Pennycuick (1989).

Sandy Key and the neighbouring Carl Ross Key, and propped in an upright position. Airspeeds were measured by ornithodolite as described by Pennycuick (1982*a,b*), but using an Epson PX-8 laptop computer to control the instrument (Pennycuick, 1987). The ornithodolite was mounted in the cockpit, and the anemometer was mounted on a pole fixed to the end of the boom, about 4.1 m above water level. The computer calculated and displayed speeds immediately, and also recorded the data on its built-in microcassette recorder. The data files were later copied to disc files, for analysis by the same computer.

#### *Video observations*

Video recordings were made at high water, with the boat anchored on the flight line used by the majority of arriving or departing birds. It was unavoidable that video recordings and speed measurements were made at different times, but there was no reason to believe that this would bias the results in any way. Recordings were made with a Panasonic PV-320 VHS camcorder, using the 'high-speed shutter' feature, which exposed each frame of the video recording for 1 ms. When single frames were played back for analysis, this was found to be very effective in 'stopping' the wings of birds in flapping flight.

#### *Measurement of span ratio*

Video sequences showing a bird flying directly towards the observer were needed for span-ratio measurements. Only a few sequences were obtained, in which the bird approached closely enough for satisfactory measurement, before turning aside to avoid the boat. A copy of the field tape, to which frame numbers

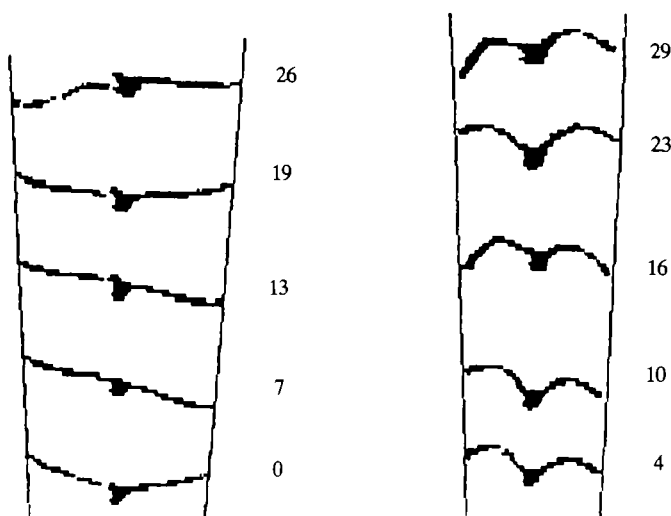


Fig. 3. Video images of a double-crested cormorant flying towards the camera, covering a period of just under 1 s. Each frame (as numbered) represents 1/30 s. Separate regressions of apparent wing span *versus* frame number were carried out for the downstrokes (left) and the upstrokes (right). Because each wingbeat cycle lasts just over six frames, there is some variation of phase in successive upstrokes and successive downstrokes.

had been added, was played back on a Panasonic PV-8000 recorder, in frame-advance mode. The video signal was passed *via* a genlock device to a Commodore Amiga computer running Deluxe Paint II (Electronic Arts), and displayed as the background to the picture. The 'coordinates' feature of Deluxe Paint II allowed the wing span of the image to be directly measured (in pixels), by moving the cursor from one wing tip to the other. The wing span was measured on selected frames near the mid-points of the upstroke and downstroke in successive wing beats (Fig. 3). The wing spans of the images measured from 22 to 54 pixels on the upstroke, where the wing tip was usually well-defined, and from 38 to 79 pixels on the downstroke, where the wing tip was sometimes difficult to locate (see Discussion). As the wingbeat frequency of this species in level flight is a little under 5 Hz, and the video frame rate under the American NTSC standard is 30 Hz (actually 29.98 Hz as observed by recording a stopwatch), each wingbeat cycle lasted for about six frames. The upstroke and downstroke were of approximately equal duration, each usually lasting for three frames. The small number of frames per cycle resulted in some unavoidable variation in the exact phase at which the span measurement was made, from one wing beat to the next.

The images in Fig. 3 were taken from one of the sequences used for finding the span ratio. They cover a period of about 1 s, and show five successive upstrokes and downstrokes. The boundary lines show in a qualitative way how the apparent wing span of the image increases from one wingbeat to the next, as the bird approached the camera. On the last upstroke the bird had begun to veer off to the

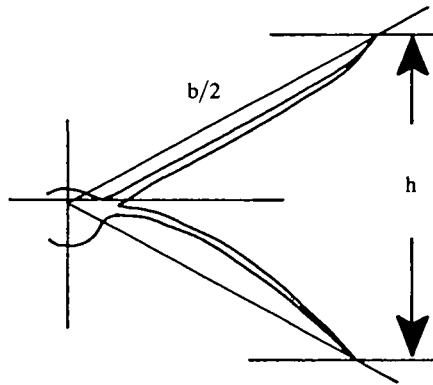


Fig. 4. The vertical excursion of the wing tip ( $h$ ) was estimated by adding together upward and downward excursions, from different video frames (drawn from two superimposed video images).  $b$  is wing span.

side, which would eventually cause the apparent wingspan to decrease, even though the bird was still coming closer. Analysis was discontinued as soon as this change in orientation became apparent. The span ratio was approximated by calculating two linear regressions, one for upstroke span against frame number, and the second for downstroke span against frame number. The span ratio was then determined by comparing the regression estimates at the frame number for the first wing beat and the last, and taking the mean of the two estimates.

#### *Measurement of lift angle*

Lift angle could not be measured directly, but an upper limit could be put on its value (see Discussion). For this, the vertical excursion of the wing tip had to be estimated. This was done from the same video recordings as those used for measuring span ratio, but choosing frames in which the wings were near the top or bottom of the downstroke, rather than at mid-stroke. The 'up-angle' between a line joining the wing tip to the shoulder joint and one passing through both shoulder joints, was measured as shown in Fig. 4, and the 'down-angle' similarly. Again, measurements were made in pixels, using the coordinates feature of Deluxe Paint II, with allowance for the different horizontal and vertical extent of each pixel. These angles were converted into an upward and downward excursion of the wing tip by assuming that the distance from shoulder joint to wing tip was equal to half the wing span (neglecting the distance separating the shoulder joints). The sum of the upward and downward excursions was the *vertical excursion* of the wing tip ( $h$ ).

## **Results**

### *Airspeed*

Fig. 5 shows the distribution of 136 ornithodolite measurements of the airspeeds

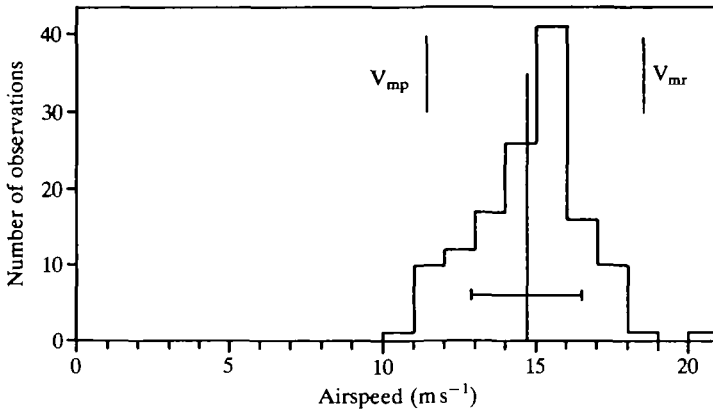


Fig. 5. Airspeed distribution for 136 ornithodolite observations. The mean airspeed (vertical bar) was  $14.7 \text{ m s}^{-1}$ , and the standard deviation (horizontal bar) was  $1.8 \text{ m s}^{-1}$ . Minimum power speed ( $V_{mp}$ ) and maximum range speed ( $V_{mr}$ ) are indicated.

of birds that were, to all appearances, proceeding steadily in level, cruising flight. The mean airspeed was  $14.7 \text{ m s}^{-1}$ , and the standard deviation was  $1.8 \text{ m s}^{-1}$ . The calculated minimum power speed ( $V_{mp}$ ) and maximum range speed ( $V_{mr}$ ) are marked, using default values in the power calculation (see below). This speed distribution does not show the anomaly noted in the closely related shag (*Phalacrocorax aristotelis*), which was reported to fly more slowly, in relation to the calculated speeds, than other northern seabirds (Pennycuik, 1987). This was tentatively attributed to lack of muscle power, preventing the shag from flying much faster than its minimum power speed. This argument would not apply to the present species, which does not have such extremely short wings (relative to its body mass) as either the shag or the southern blue-eyed shag (*P. atriceps*). The latter species has a slightly shorter wing span than the double-crested cormorant, but almost twice the mass, and the shag is similarly proportioned.

#### Span ratio and lift angle

The span ratio given in Table 1 is a mean value from three video sequences, totalling 28 wingbeats. The value for the lift angle is a maximum figure, derived as shown in Fig. 6. The wing is assumed to sweep from the fully up position to the fully down position, while the bird travels forwards a distance  $\lambda/2$ , where  $\lambda$  is the *flapping wavelength*, defined as:

$$\lambda = V/f, \quad (7)$$

$V$  being the airspeed and  $f$  the flapping frequency. The wing tip descends through a distance  $h$  (see above). As long as the wing up- and down-angles are not too large, the wing-tip path can be represented as approximately linear, as seen from the side, and descending at an angle  $\theta$  to the horizontal. Clearly the lift angle ( $q$ ) cannot exceed  $\theta$ . If the lift force acting on the whole wing could be represented as a vector average, it would appear to act some distance in from the wing tip, where

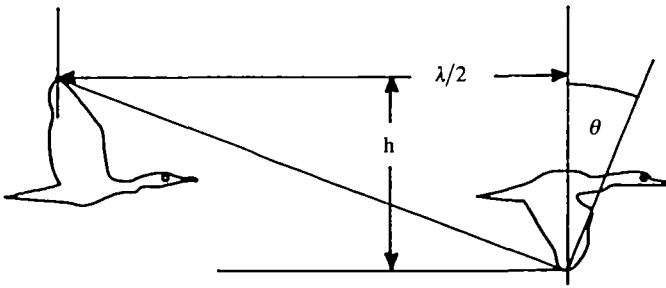


Fig. 6. The angle  $\theta$  is calculated on the assumption that the wing tip descends linearly through its vertical excursion ( $h$ ) during the downstroke, while the bird moves forward a distance equal to half the flapping wavelength ( $\lambda$ ).  $\theta$  is a maximum estimate for the lift angle ( $q$ ).

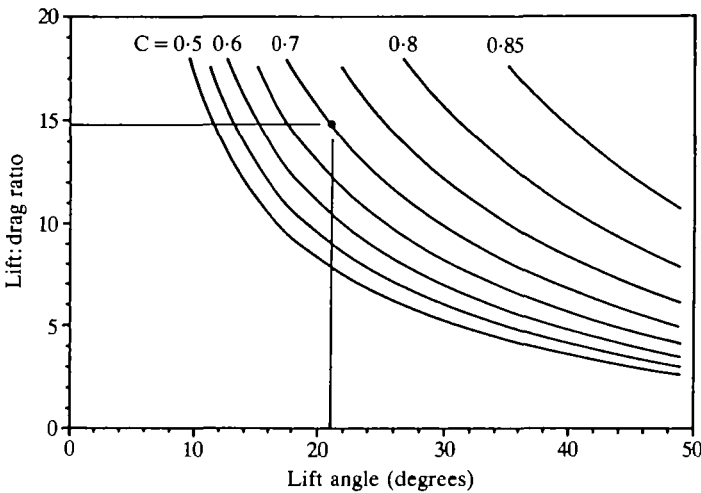


Fig. 7. Effective lift:drag ratio plotted against lift angle, for various values of the span ratio ( $C$ ), from equation 5. The point represents the field results on the double-crested cormorant.

the vertical excursion is less than  $h$ , so that the practical value of  $q$  must be somewhat less than  $\theta$ .

### Discussion

According to equation 5, the figures in Table 1 should suffice to estimate the effective lift:drag ratio ( $N$ ), remembering that the value given for the lift angle is actually the angle labelled  $\theta$  in Fig. 6, and is a maximum estimate for  $q$ . Fig. 7 shows plots (from equation 5) of  $N$  versus  $q$ , for various values of the span ratio ( $C$ ). The point corresponds to the values of  $C$  and  $q$  in Table 1. The resulting estimate of  $N$  is 14.8. The slopes of the lines in Fig. 7 show that if the true value of  $q$  were lower, then the estimate of  $N$  would be even higher.

This may be compared with the estimate of  $N$  obtained by calculating a power curve according to the methods of Pennycuick (1975). This was done by inserting the body mass and wing span from Table 1 in one of the BASIC programs published by Pennycuick (1989). The particular version of the power curve used was program 1A, in which the total power required to fly is calculated as the sum of induced, profile and parasite powers; that is, as the sum of the mechanical components of power, excluding basal metabolism and other 'metabolic' components. Using the default values in the program, which are those recommended by Pennycuick (1975), the maximum effective lift: drag ratio was estimated as 8.96, which is only about two-thirds of the estimate from the span-ratio observations. The discrepancy could be due to an overestimate of the power by the computer program, or to upward bias in the estimate of  $N$  from the field observations, or to a combination of both. An overestimate of the computed power could be due to an overestimate in any or all of the three components that contribute to the total power; that is induced, profile and parasite powers.

#### *Induced power*

The induced power is calculated in the program from a simple momentum-jet theory, which is thought to under- rather than overestimate the power. Because of this, the initial result is multiplied by an 'induced power factor' ( $k$ ), representing the fact that the bird's vortex wake supports the weight less efficiently than the ideal momentum jet. The default value used for  $k$  in the program is 1.2; that is, the induced power is increased by 20% to allow for the inefficiency of the lift-generation process. In the case of a bird flying with a concertina wake, this allowance may be excessive. An additional reason why induced power might have been less than that estimated is that many of the birds were flying very low, over a smooth water surface, and may have been within the influence of ground effect. According to Blake (1983), a bird gliding at a height equal to half its wing span might expect a reduction of 20% in its induced drag, and there would probably be a similar reduction in induced power in flapping flight. Thus, under the conditions of observation, it is possible that a value of 1.1 for  $k$  would have been more realistic than 1.2, and a value of 1.0 is conceivable.

#### *Profile power*

Profile power in the program is regarded as independent of speed. This approximation is only recommended for speeds from the minimum power speed to the maximum range speed. Subject to this restriction, the profile power is found as a fixed multiple ( $X_1$ ) of the 'absolute minimum power'; that is the sum of induced and parasite powers at the minimum power speed. The rationale for this is explained by Pennycuick (1975). The default value for  $X_1$  is 1.2, but the empirical basis for this is slender. It is readily conceivable that the real value of  $X_1$  could be considerably lower (or higher) than assumed.

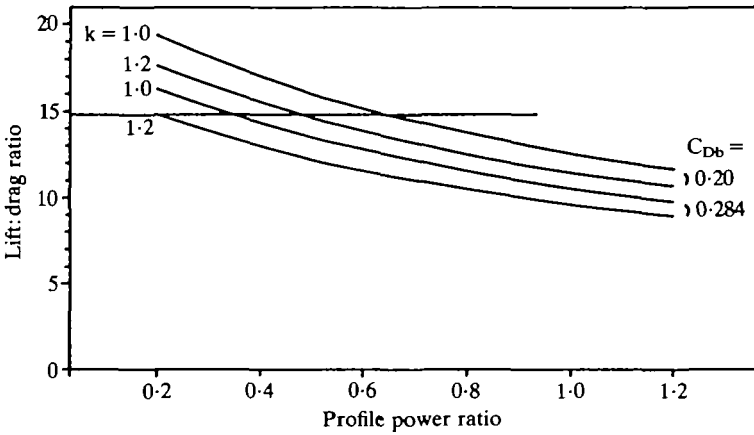


Fig. 8. Effective lift:drag ratio for the double-crested cormorant, calculated from program 1A of Pennycuick (1989), with various values for the profile power ratio, induced power factor ( $k$ ), and body drag coefficient ( $C_{Db}$ ). The horizontal line at  $N = 14.8$  is the value from Fig. 7.

#### *Parasite power*

Parasite power is estimated from the body frontal area and drag coefficient, which are themselves estimated from the mass by a method based on the wind-tunnel results of Pennycuick *et al.* (1988). Details of the calculation are given by Pennycuick (1989). The experimental measurements were made on bird bodies from which the wings had been removed, and there are indications that the boundary layer separated more readily from the downstream ends of these bodies than it would do from an intact bird in flight. These doubts are discussed by Pennycuick (1989), and lead to suspicions that the estimated body drag coefficient ( $C_{Db}$ ) may be too high.

#### *Effect of modifying default values*

Program 1A of Pennycuick (1989) was designed to be run repeatedly, with systematic changes in the values of variables. The program was run 24 times, with  $k$  set to alternative values of 1.2 and 1.0, with six values of  $X_1$  from 1.2 to 0.2, and with  $C_{Db}$  set first to 0.284 (the value calculated automatically from the mass) and then to 0.20, which was considered an extreme low value. The values of the effective lift:drag ratio ( $N$ ) that resulted are plotted as a family of curves in Fig. 8. The value found from the span-ratio observations (14.8) is marked as a horizontal line. Fig. 8 shows that even if the extreme low values are chosen for the induced power factor and body drag coefficient, the profile power ratio still has to be nearly halved to bring the predicted value of  $N$  into line with the estimate from the span-ratio observations. Although it is conceivable that such drastic adjustments to the power calculation really are necessary, the discrepancy could also be due to some error in the span-ratio measurements or calculation, which has caused the result to be biased upwards.

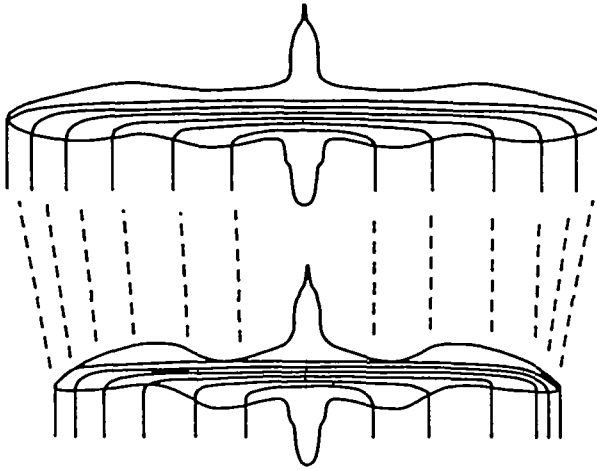


Fig. 9. The spanwise distribution of lift is represented by the shedding of vortex lines along the trailing edge. The lift per unit span at any point is proportional to the number of vortex lines attached to the wing at that point. It is assumed here that the lift distribution remains the same when the wing is shortened (left-hand side). If the vortex lines were more bunched towards the tip when the wing is shortened (right-hand side), more lift would be developed than with the distribution shown at left.

#### *Spanwise lift distribution*

The explanation of the concertina wake given by Pennycuik (1988) represents the bound vortex as a single vortex, extending from wing tip to wing tip, and then bending around to continue as a pair of trailing vortices. In fact, vorticity is shed as a continuous vortex sheet from the whole of the trailing edge. This is usually represented diagrammatically as in Fig. 9, by showing the bound vortex as made up from a number of vortex lines, each extending over only part of the span. Each vortex line makes a contribution to the lift in proportion to the amount of the span that it covers before it leaves the wing at the trailing edge. The lift per unit span dwindles towards the wing tip, in proportion to the number of vortex lines still attached to the wing. The assumption implicit in the span-ratio calculation above, and also in Rayner's (1986) theory of the constant-circulation wake, is that the spanwise distribution of the lift (as determined by the distribution of vortex shedding) has the same shape on both the upstroke and the downstroke, as in Fig. 9 (left). There is no means of checking this assumption. One could imagine, for example, that the vortex lines might be more bunched towards the wing tip when the wing span is reduced, as suggested in Fig. 9 (right). In this case the lift would not be reduced in direct proportion to the wing span, as assumed above. The lift developed during the upstroke would be greater than that estimated under this assumption. The effect would be that the real value of the effective lift:drag ratio would be higher than the estimate. The opposite bias is required to account for the discrepancy noted above, meaning that more vortex lines would have to be shed close to the body during the upstroke. Although this seems difficult to

imagine, it is a possibility that could be borne in mind if the discrepancy remains intractable.

#### *Visibility of wing tips*

A more likely source of bias is a tendency to 'lose' the wing tips on the video image during the downstroke. When the bird is viewed from ahead, the wing tips are seen edge-on during the downstroke, whereas they present a bolder image when the wing is rotated nose-up during the upstroke (Fig. 3). If contrast is poor, because the bird is distant or the lighting is flat, the wing span is more likely to be underestimated on the downstroke than on the upstroke. This causes a tendency to overestimate the span ratio, and hence also the lift:drag ratio (Fig. 7). Some bias from this cause is possible, but hardly the 50 % upward bias noted above as necessary to reconcile the observations with the output of the power calculation.

#### *Conclusion*

Taking into account likely sources of bias in the span-ratio observations, it still appears that the power estimated by the computer programs of Pennycuick (1989) is on the high side. It is to be hoped that the publication of these programs will stimulate investigators to devise further field or laboratory observations that can be compared with the predictions. If a consensus emerges that the power estimates need to be revised downwards, then other considerations will have to be brought to bear to determine which parts of the calculation require revision.

It is a pleasure to thank the authorities of the Everglades National Park for their helpful cooperation. I am also indebted to Sea and Sky Foundation for equipment and facilities.

#### **References**

- BLAKE, R. W. (1983). Mechanics of gliding in birds with special reference to the influence of the ground effect. *J. Biomechanics* **16**, 649–654.
- PENNYCUICK, C. J. (1975). Mechanics of flight. In *Avian Biology*, vol. 5 (ed. D. S. Farner & J. R. King), pp. 1–75. New York: Academic Press.
- PENNYCUICK, C. J. (1982a). The ornithodolite: an instrument for collecting large samples of bird speed measurements. *Phil. Trans. R. Soc. Ser. B* **300**, 61–73.
- PENNYCUICK, C. J. (1982b). The flight of petrels and albatrosses (Procellariiformes), observed in South Georgia and its vicinity. *Phil. Trans. R. Soc. Ser. B* **300**, 75–106.
- PENNYCUICK, C. J. (1987). Flight of auks (Alcidae) and other northern seabirds compared with southern Procellariiformes: ornithodolite observations. *J. exp. Biol.* **128**, 335–347.
- PENNYCUICK, C. J. (1988). On the reconstruction of pterosaurs and their manner of flight, with notes on vortex wakes. *Biol. Rev.* **63**, 299–331.
- PENNYCUICK, C. J. (1989). *Bird Flight Performance. A Practical Calculation Manual*. Oxford: Oxford University Press.
- PENNYCUICK, C. J. & LOCK, A. (1976). Elastic energy storage in primary feather shafts. *J. exp. Biol.* **64**, 677–689.
- PENNYCUICK, C. J., OBRECHT, H. H. & FULLER, M. R. (1988). Empirical estimates of body drag of large waterfowl and raptors. *J. exp. Biol.* **135**, 253–264.
- RAYNER, J. M. V. (1986). Vertebrate flapping flight mechanics and aerodynamics, and the evolution of flight in bats. *Biona Report* **5**, 27–74.

- SPEDDING, G. R. (1981). The vortex wake of flying birds: an experimental investigation. PhD thesis, University of Bristol.
- SPEDDING, G. R. (1987). The wake of a kestrel (*Falco tinnunculus*) in flapping flight. *J. exp. Biol.* **127**, 59–78.
- SPEDDING, G. R., RAYNER, J. M. V. & PENNYCUICK, C. J. (1984). Momentum and energy in the wake of a pigeon (*Columba livia*) in slow flight. *J. exp. Biol.* **111**, 81–102.

